

THE INFLUENCE OF THE OXIDATION DEGREE OF BISMUTH OXIDE THIN FILMS ON THEIR OPTICAL PROPERTIES

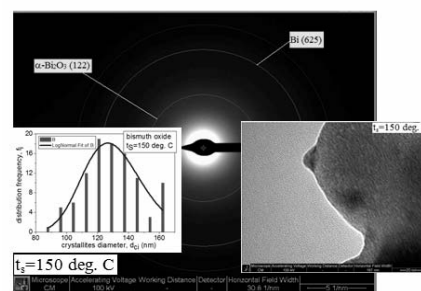
Simona CONDURACHE-BOTA^a and Nicolae TIGAU^{a, b}

^a Faculty of Sciences and Environment, Dunarea de Jos University of Galați, 111 Domneasca Street, 800201 Galați, Roumania

^b Center of Nanostructures and Functional Materials-CNMF, Dunarea de Jos University of Galați, 111 Domneasca Street, 800201 Galați, Roumania

Received September 23, 2016

Despite their often complicated structure, bismuth oxide thin films are still of interest due to several properties, such as: semiconducting behavior with large energy bandgap, high refractive index and gas sensitivity. Thermal oxidation is one versatile method for the preparation of bismuth oxide from pure bismuth films. But, while oxidizing, bismuth can form several non-stoichiometric oxides except for bismuth trioxide, the latter exhibiting complicated polymorphism and polycrystallinity. This is why in-depth structural analysis is needed in order to properly interpret the properties of such films. Transmission electron microscopy (TEM) is the method of choice for this purpose. Here we propose a TEM morpho-structural analysis of highly transparent bismuth oxide thin films deposited on glass substrates at two different temperatures, along with their optical analysis, revealing their high energy band gap, with low sensitivity to the oxidation degree, which, instead, strongly influences their refractive indexes and absorption coefficients.



INTRODUCTION

Semiconducting films can be prepared by thermal oxidation of pure metal films, as it is a versatile and cheap method. As expected, the deposition conditions of the pure metal films strongly influence the final oxide films, along with the oxidation conditions. In the case of bismuth, its oxidation often leads to complicated compositions and structures, due to the coexistence of two or more of its 8 stable intermediate oxides (BiO , $\text{BiO}_{1.5}$, $\text{Bi}_2\text{O}_{2.33}$, $\text{Bi}_2\text{O}_{2.5}$, $\text{Bi}_2\text{O}_{2.7}$, Bi_2O_4 , Bi_4O_7 and $\text{Bi}_{12.8}\text{O}_{19.2}$), with their different crystalline systems and of some of the 7 forms of bismuth trioxide, Bi_2O_3 , *i.e.* the stoichiometric oxide.^{1,2} Even though for such a mixture of oxides within the same film, it is harder to correlate the composition and structure with the properties of the film, on the

other side, depending on the coexisting oxides, the overall film might exhibit specific and useful properties. This is the case in this paper, where the particular mixtures of oxides within two types of bismuth oxide films obtained by thermal oxidation in air of pure bismuth films exhibit large energy bandgap for the typical indirect allowed transitions of such films, in a somehow opposite manner with other films made of bismuth oxide mixtures, which have very low energy bandgaps.¹

In any of their mixed compositions, bismuth oxide films prepared by different methods have already proved their potential for various applications (gas sensing, solar cells, optical coatings, ceramic glass manufacturing, fuel cells, etc.).³⁻⁹

Thus, the proper knowledge of the in-depth composition and structure of such mixed films allows for the good interpretation and correlation

* Corresponding author: scondurache@ugal.ro

with and between their various physical properties. Transmission Electron Microscopy (TEM) with the SAED (Selected Area Electron Diffraction) technique is the method of choice when in-depth composition and structure of thin films are concerned. Also, bright-field TEM (BF-TEM) images allow for the study with the highest magnification of the crystalline grains and of their distribution within the films. These were the chosen methods for the bismuth oxide films analyzed here. And since Optoelectronics can take advantage of the properties of bismuth oxide films, the most relevant optical properties of the chosen samples (*i.e.* two types of bismuth oxide thin films prepared by thermal oxidation in air of pure bismuth thin films thermally-deposited in vacuum on glass substrates maintained at 2 different temperatures, namely at $t_s = 50$ deg. C and at $t_s = 150$ deg. C, respectively) were analyzed and correlated with their composition, structure and grain distribution, along with the preparation conditions used for each type of film under study.

RESULTS AND DISCUSSION

Fig. 1 presents the SAED images allowing for the identification of the composing oxides within the analyzed films. It can be easily noticed that the film obtained by thermal oxidation in air of a pure bismuth thin film deposited by thermal vacuum evaporation at $t_s = 150$ deg. C of the substrate temperature presents a simple composition, made of the monoclinic alpha-form of bismuth trioxide and some unoxidized bismuth. Within this film, each component presents only one type of crystalline plane.

Instead, the film obtained by thermal oxidation in air of a pure Bi film deposited by thermal vacuum evaporation at only 50 deg. C of the substrate temperature, shows an extremely complicate composition and structure. Thus, this film proves to be a mixture made of:

- i) unoxidized bismuth with coexisting 5 types of crystalline planes (*i.e.* polycrystallinity);
- ii) 5 types of non-stoichiometric bismuth oxides, from which $\text{Bi}_2\text{O}_{2.75}$ and $\text{Bi}_2\text{O}_{2.33}$ are present each with 3 types of crystalline planes;
- iii) 3 forms of the stoichiometric bismuth trioxide, namely: the monoclinic alpha, $\alpha\text{-Bi}_2\text{O}_3$, the tetragonal beta, $\beta\text{-Bi}_2\text{O}_3$ and the volume-centered cubic gamma, $\gamma\text{-Bi}_2\text{O}_3$ (polymorphism), from which the first two are present with two types of crystalline planes each.

The initial bismuth films were structurally analyzed prior to their thermal oxidation and showed similar structures,¹⁰ namely Bi was present in both films with 8 crystalline planes: (222), (116), (012), (104), (003), (107), (110) and (015), while only the 1st film (that with $t_s = 50$ deg. C during the deposition) presented also the (331), $(2\bar{1}1)$ and (200) planes, whilst the 2nd film (that with $t_s = 150$ deg. C during the deposition) also contained the (027), (310), (018), (122), (220) and (202) planes, as studied elsewhere.¹⁰ It has to be pointed out that no bismuth oxide was identified in the film deposited at higher temperature, following the structural analysis,¹⁰ instead one intermediate oxide was present in the film deposited at 50 deg. C, namely $\text{Bi}_2\text{O}_{2.7}$.¹⁰ We must mention here that except for the glass substrates temperatures during the initial pure bismuth thin films depositions, the rest of the deposition and subsequent thermal oxidation conditions were kept the same for the two types of films under study. Still, the SAED analysis showed that 100 deg. Celsius difference between the substrate temperatures during the deposition of the two types of bismuth films led to very different composition and structures of the films upon thermal oxidation in air, which also explains their rather different thicknesses, namely 0.26 μm for the bismuth oxide film with $t_s = 50$ deg. C and 0.6 μm for the bismuth oxide film with $t_s = 150$ deg. C. Thus, when oxidizing pure bismuth films in air at high temperatures (400 deg. C in our case), the oxygen uptake differs significantly if the structures of the initial films are only slightly different. The oxidation process of polycrystalline metallic films is complicated, since the oxygen adsorption and its penetration between multiple crystalline planes depends on their density and relative orientation and, subsequently, on the number and dimensions of the free channels in-between. In our case, when heating pure bismuth films up till 400 deg. C, the structure simplified significantly only in the case of the 2nd film, leading to only one crystalline plane for bismuth trioxide (namely the (122)) and one for the remaining unoxidized Bi (namely plane (625)). Instead, the 1st film proved to have a more complicated structure than the source film (*i.e.* the pure Bi film deposited at 50 deg. C).

The bright-field TEM images of the two films are presented in Fig. 2, showing that the films are composed of big grains on a continuous background, the latter being due to bismuth incomplete oxidation.

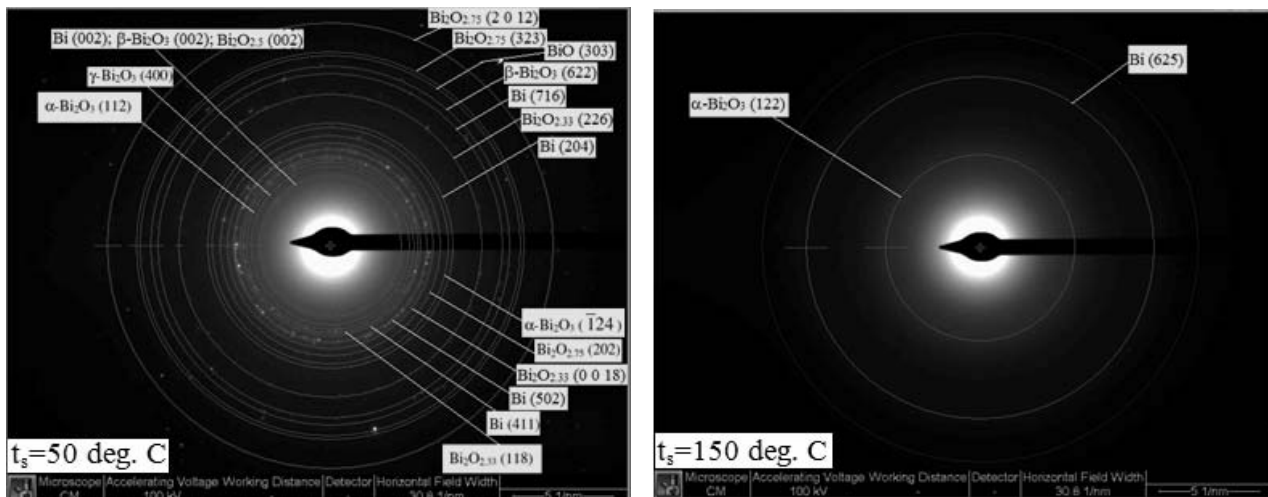


Fig. 1 – SAED images for the bismuth oxide thin films under study

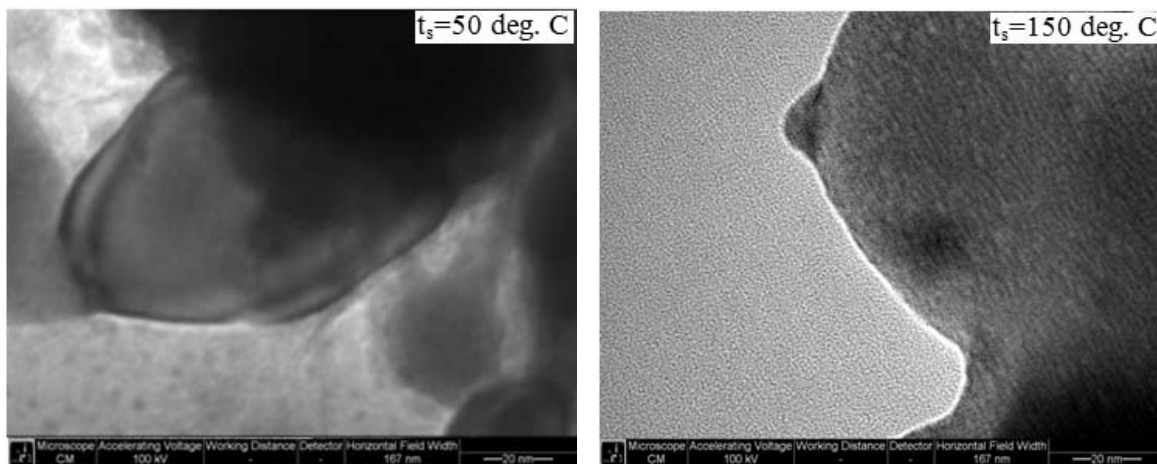


Fig. 2 – BF-TEM images of the investigated bismuth oxide thin films.

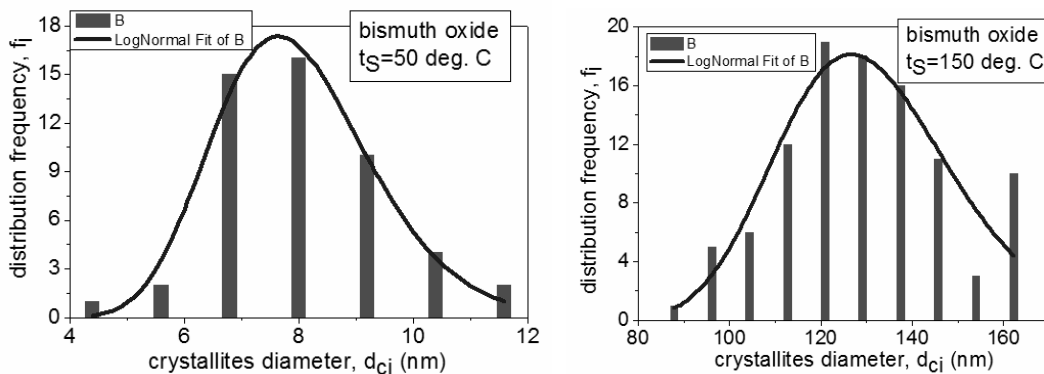


Fig. 3 – Grain distribution and Lognormal fitting for each of the studied films.

The grain statistics for size and shape based on the TEM images proved that the grain histograms can be well fitted with the Lognormal function (see Fig. 3), which is typical for thin films and prove their uniform grain distribution.

Table 1 presents the most relevant morphological parameters of the bismuth oxide crystalline grains as

inferred from the TEM images, namely their average diameter and average sphericity. Whilst the sphericity is the same for both films, instead, the average diameter of the bismuth oxide films with $t_s = 150 \text{ deg. C}$ is 16 times bigger than for the film with $t_s = 50 \text{ deg. C}$.

Table 1

Morphological parameters of the bismuth oxide crystalline grains as inferred from the TEM images

t_s (deg. C)	50	150
Average diameter (nm)	8.04	128.91
Average sphericity	0.68	0.68

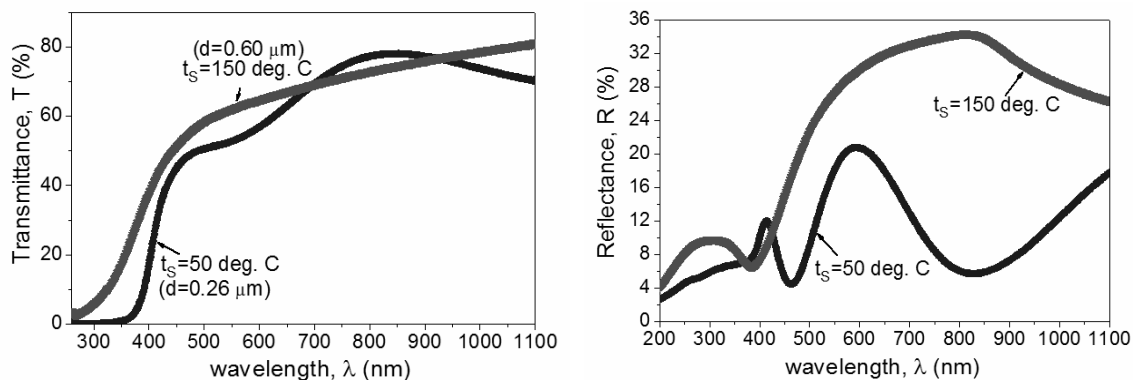


Fig. 4 – The optical measurements for the bismuth oxide thin films under study.

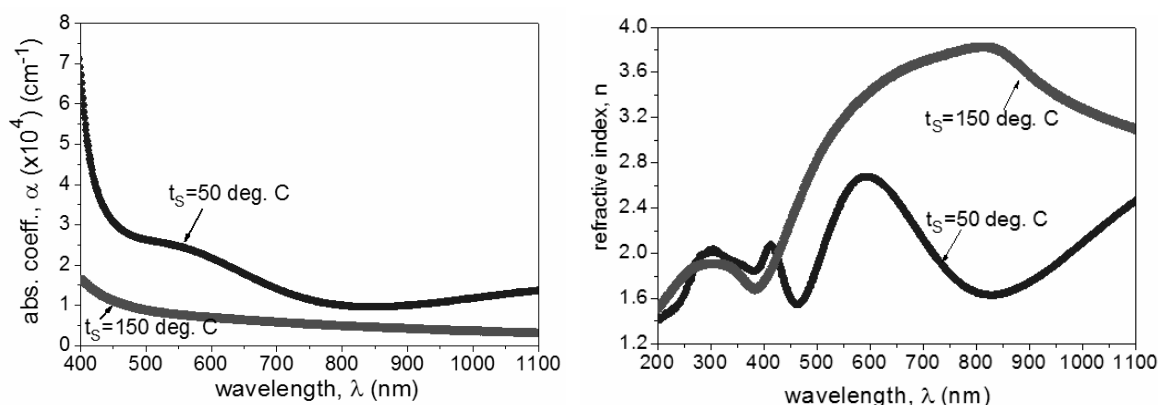


Fig. 5 – The computed refractive indexes and absorption coefficients of the investigated films in the NIR-VIS-NUV range.

The optical transmittance and reflectance spectra as measured for the bismuth oxide films under study are showed in Fig.4, exhibiting that the films are highly transparent above 450 nm, with more than 50 % transmittances, while the reflectance is higher for the oxide film with $t_s = 150$ deg. C for almost the entire investigated spectral range (200-1100 nm). As it can be seen in Fig. 4, the reflectance is more sensitive (*i.e.* changes more) with the oxidation degree of the bismuth oxide films than the optical transmittance, even though the films have significantly different thicknesses. It is to be expected that the reflectance of polymorph and polycrystalline oxide films to strongly depend on the type of composing crystalline planes, since the reflection process depends on the orientation of these planes and on the position and density of the atoms within them.

The absorption coefficient and the refractive index and were computed for each wavelength and each film, along with the optical energy bandgap for each type of electronic transition (see Tauc's formula with the 'r' coefficient indicating the type of transition) from the optical transmittance and reflectance experimental data, according to typical formulas given elsewhere.¹¹ The results are presented in Fig. 5 and Table 2. The graphs from Fig. 5 show higher absorption coefficients for the film with $t_s = 50$ deg. C than for the one with $t_s = 150$ deg. C. Thus, a complex composition and structure of the oxidized bismuth films leads to a higher absorption of visible and near-infrared radiation, as it is the case here for the 1st film (the one with $t_s=50$ deg. C).

Table 2

Optical energy band gap of the studied films

t_s (deg. C)	Indirect allowed transitions ($r = 1/2$)	Direct allowed transitions ($r = 2$)	Direct forbidden transitions ($r = 1/3$)	Indirect forbidden transitions ($r = 2/3$)
50	3.09	2.18	1.54	2.48
150	3.05	2.11	1.64	2.41

The refractive index respects the trend with wavelength of the optical reflectance, on which it depends much more than on the optical transmittance. Above 500 nm, the refractive index of the film with $t_s = 150$ deg. C surpasses the value of 3, while the oxide film that comes from pure Bi deposited at 50 deg. C doesn't surpass the value of 2.5, given its more complicated structure. Spectral regions with anomalous dispersion for the refractive index are found for both films, recommending them for optical applications.

The energy bandgap lies around 3.07 eV for both films in the case of their typical electronic transitions, namely those of indirect allowed-type. The energy bandgaps for the other three types of transitions are also very similar for both films, proving the insensitivity of this crucial optoelectronic parameter to the oxidation degree of the bismuth oxide films.

EXPERIMENTAL

Pure (99.99 %) bismuth powder from Merck was deposited as thin films onto glass substrates, by thermal

vacuum evaporation from quartz crucibles introduced into tantalum coil evaporators crossed by 10 A electrical current. The depositions took place at $5 \cdot 10^{-5}$ torr within the stainless steel, cylindrical preparation chamber (see Fig. 6 for the image of the deposition device type AV 1003).

During the depositions, the substrates were kept at different temperatures. We analyze here the films deposited at 50 and 150 deg. C, respectively. After cooling and extraction from the deposition chamber, the bismuth films were submitted to thermal oxidation in air with $\cong 11.2$ deg. C/min, up till 400°C, for 1 hour total heating – cooling cycle. The cooling rate was $\cong 20$ deg. C /min. A home-made annealing device was used for the oxidation process.

Transmission electron microscopy (Philips CM120ST TEM device) was used in order to obtain high magnification images of the films (BF-TEM technique), along with the in-depth morphological analysis of the grain distribution, while the associated SAED - Selected Area Electron Diffraction – technique was employed for structure identification.

A MII-4 Linnik interferential microscope was used for the thickness measurements by white-light interferometry. Optical transmittance and reflectance measurements were carried out at a Perkin Elmer Lambda 35 Spectrometer, for the 200 – 1100 nm spectral range. From the experimental data, the absorption coefficients, the refractive indices and the optical energy bandgaps of the films were computed.

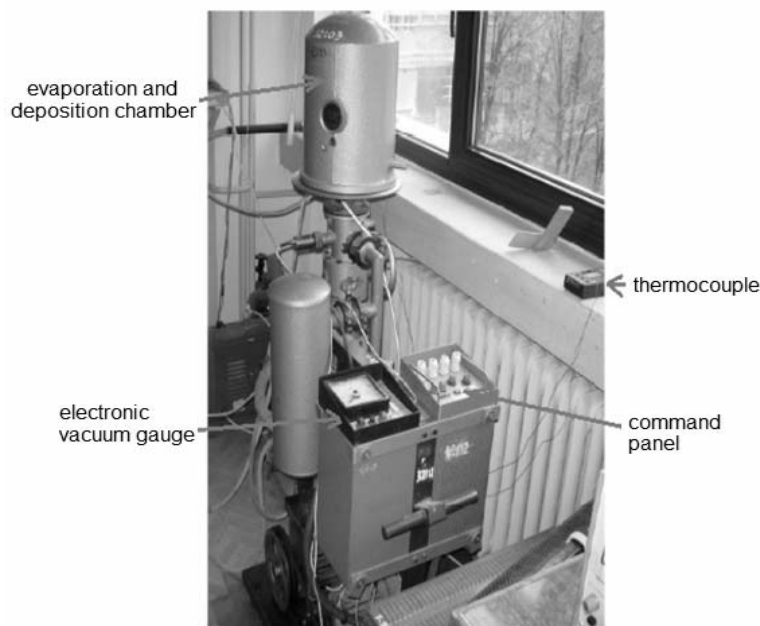


Fig. 6 – The image of the thermal evaporation device used for film deposition.

CONCLUSIONS

Bismuth oxide films with different oxidation degrees were compared in terms of their composition, structure and optical properties. It was found that the composition and the structure of the oxidized films are highly sensitive to the substrate temperature during initial bismuth films deposition. The in-depth TEM imaging revealed higher grains for 100 deg. higher substrate temperature during the initial bismuth deposition.

Both analyzed films exhibited high transmittance, even though their thicknesses were very different. The reflectivity and the refractive index are higher for the film with $t_s=150$ deg. C, while the absorption coefficient was higher for the film deposited at the lower substrate temperature ($t_s=50$ deg. C), with more oxides within its composition. The films present semiconductor behavior, with optical bandgaps rather insensitive to the oxidation degree of each film, for all types of electronic transitions.

The films require structural stabilization through annealing, after which such highly-transparent, semiconducting films will be useful for various optoelectronic applications.

REFERENCES

1. S. Condurache-Bota, C. Constantinescu, N. Țigău and M. Praisler, *Surf. Rev. Lett.*, **2015**, 23, 1550104.
2. JCPDS data files nos. 01-0688, 05-0519, 18-244, 27-49, 27-50, 27-51, 27-52, 27-54, 29-236, 41-1449, 44-1246, 45-1344, 47-1057, 47-1058, 71-0465, 71-0466, 71-0467, 71-2274, 72-0398, 74-1373, 74-1375, 74-1633, 74-1999, 74-2352, 75-0993, 75-0995, 76-1730, 77-0374, 77-0868, 77-2008, 78-0736, 81-0563, 83-0410, 85-1329.
3. C.M.B. Hincapié, M.J.P. Cárdenas, J.E.A. Orjuela, E.R. Parra and J.J.O. Florez, *Dyna*, **2012**, 176, 139-148.
4. C. L. Gomez, Osmar Depablos-Rivera, P. Silva-Bermudez, S. Muhl, A. Zeinert, M. Lejeune, S. Charvet, P. Barroy, E. Camps and S. E. Rodil, *Thin Solid Films*, **2015**, 578, 103–112.
5. F. Schroder, N. Bagdassarov, F. Ritter and L. Bayarjargal, *Phase Transit.*, **2010**, 83, 311–325.
6. R. B. Patil, R. K. Puri and V. Puri, *Appl. Surf. Sci.*, **2007**, 253, 8682-8688.
7. J. Morasch, S. Li, J. Brotz, W. Jaegermann and A. Klein, *Phys. Status Solidi A*, **2014**, 211, 93–100.
8. S. S. Bhande, R.S. Mane, A. V. Ghule and S.-H. Han, *Scripta Mater.*, **2011**, 65, 1081–1084.
9. C.-H. Ho, C.-H. Chan, Y.-S. Huang, L.-C. Tien and L.-C. Chao, *Opt. Express*, **2013**, 21, 11965 - 11972.
10. S. Condurache-Bota, R. Drasovean, N. Tigau and A. P. Rambu, *Rev. Roum. Chim.*, **2011**, 56, 1097–1102.
11. S. Condurache-Bota, G. I. Rusu, N. Tigau and L. Leontie, *Cryst. Res. Technol.*, **2010**, 45, 503 – 511.